Supporting Information for

Solvation and Oxidation Effects on the Crystal Structure and Morphology of Tetraoxolene-Based Materials

Ashlyn A. Kamin,[†] EJ Brannan,[†] Kathleen M. Snook, Sebastian Krajewski, Paige M. Gannon, Werner Kaminsky, Dianne J. Xiao[*]

Department of Chemistry, University of Washington, Seattle, Washington 98195, USA

[†]These authors contributed equally to this work
[*]Correspondence to: djxiao@uw.edu

Table of Contents

1. General Materials and Methods:

Reactions were performed in air unless otherwise specified. Reagents and solvents were purchased from commercial vendors (Millipore Sigma, TCI America, Alfa Aesar, Fisher Scientific, Oakwood Chemical, Combi-Blocks) and used without further purification.

High-resolution combustion analysis was conducted by Atlantic Microlabs Inc. (Norcross, GA, USA).

Attenuated total reflectance infrared (ATR-IR) spectra were collected on a Perkin Elmer Frontier FT-IR/FIR instrument equipped with a diamond ATR accessory.

Scanning electron microscopy (SEM) images were collected on a ThermoFisher Scientific ApreoS with LoVac scanning electron microscope with an operating voltage of 2 kV. All samples were prepared by dropcasting from DMF or DMA suspensions onto silicon wafers and coated with Pt at a thickness of 4 nm. Particle sizes distributions were determined by measuring 100 random particles across at least five different SEM images.

2. Synthetic Procedures:

The tetraoxolene ligands, H_2Ph_2dhbq and H_4Ph_2dhbq, were synthesized as previously reported.[1]

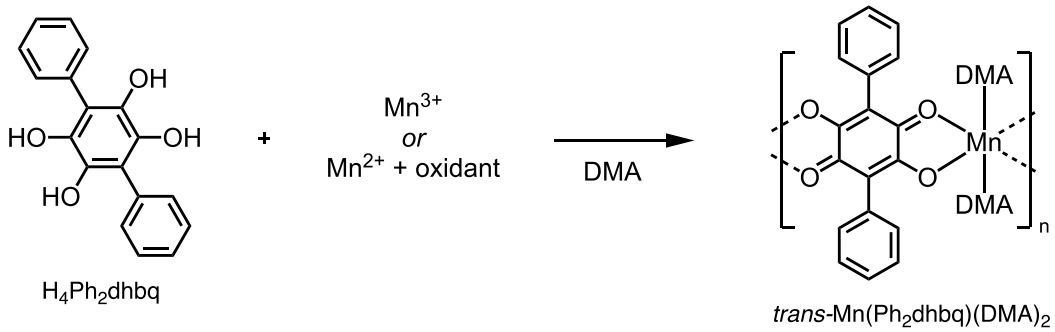

Synthesis of *trans*-Mn(Ph$_2$dhbq)(DMA)$_2$ for SCXRD: A solution of H_4Ph_2dhbq (1.25 mg, 0.004 mmol) in DMA (0.4 mL) was added to a 1 mL culture tube. A solution of $Mn(NO_3)_2{\cdot}4H_2O$ (0.80 mg, 0.003 mmol, 0.75 eq.) in MeOH (0.4 mL) was layered above the solution of H_4Ph_2dhbq. The culture tube was placed inside a 20 mL scintillation vial, capped, and allowed to sit at room temperature for 10 days to give small, dark purple crystal rods suitable for X-ray diffraction.

Synthesis of *trans*-Mn(Ph$_2$dhbq)(DMA)$_2$ in air: A solution of H_4Ph_2dhbq (94.1 mg, 0.319 mmol) in DMA (30 mL) was divided evenly amongst three 20 mL scintillation vials. A solution of $Mn(NO_3)_2{\cdot}4H_2O$ (81.4 mg, 0.324 mmol, 1 eq.) in DMA (30 mL) was added, dividing similarly between the vials. The vials were sealed and heated at 80 ˚C for two days to give small, dark purple crystals. The resulting crystals were combined and washed with DMA (3 × 20 mL) and dried under flowing nitrogen. The chain *trans*-Mn(Ph_2dhbq)$(DMA)_2$ was obtained in 50% yield (84.4 mg, 0.162 mmol). Anal. Calc. for $(MnC_{26}H_{28}N_2O_6)(DMA)_{0.15}$: C, 59.89; H, 5.52; N, 5.68. Found: C, 59.84; H, 5.42; N, 5.64.

Alternative synthesis of *trans*-Mn(Ph$_2$dhbq)(DMA)$_2$ from Mn^{III}: In a nitrogen-filled glovebox, a solution of H_4Ph_2dhbq (20.0 mg, 0.068 mmol) in DMA (4 mL) was added to a 20 mL scintillation vial. A solution of $Mn(acac)_3$ (24.2 mg, 0.069 mmol, 1 eq.) in DMA (4 mL) was added. The vial was sealed and heated at 80 ˚C for nine days to give a purple powder. The resulting powder was washed with DMA (3 × 10 mL) and dried under flowing nitrogen. The chain *trans*-Mn(Ph_2dhbq)$(DMA)_2$ was obtained in 49% yield (17.4 mg, 0.033 mmol). Anal. Calc. for $(MnC_{26}H_{28}N_2O_6)$ $(H_2O)_{0.5}(DMA)_{0.1}$: C, 59.03; H, 5.61; N, 5.48. Found: C, 59.05; H, 5.56; N, 5.55.

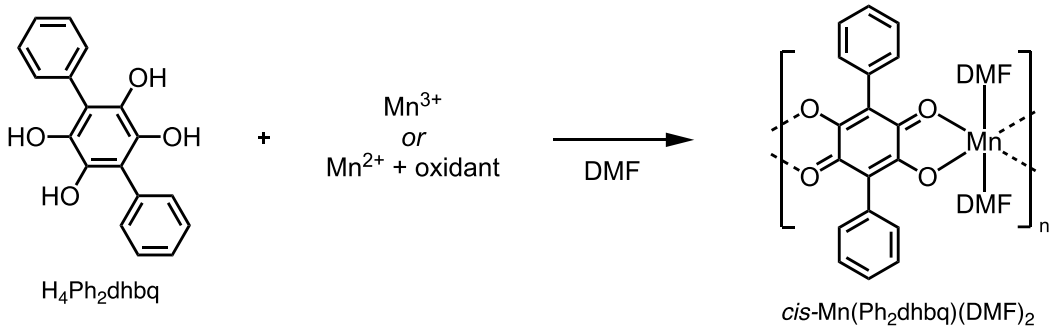

H_4Ph_2dhbq *cis*-$Mn(Ph_2dhbq)(DMF)_2$

Synthesis of *cis*-Mn(Ph2dhbq)(DMF)2 for SCXRD: A solution of H_4Ph_2dhbq (1.25 mg, 0.004 mmol) in DMF (0.4 mL) was added to a 1 mL culture tube. A solution of $Mn(NO_3)_2{\cdot}4H_2O$ (0.80 mg, 0.003 mmol, 0.75 eq.) in MeOH (0.4 mL) was layered above the solution of H_4Ph_2dhbq. The culture tube was placed inside a 20 mL scintillation vial, capped, and allowed to sit at room temperature for 10 days to give small, dark purple crystal rods.

Synthesis of *cis*-Mn(Ph2dhbq)(DMF)2: A solution of H_4Ph_2dhbq (88.8 mg, 0.302 mmol) in DMF (30 mL) was divided evenly amongst three 20 mL scintillation vials. A solution of $Mn(NO_3)_2{\cdot}4H_2O$ (78.0 mg, 0.311 mmol, 1 eq.) in DMF (30 mL) was added, dividing similarly between the vials. The vials were sealed and heated at 80 ˚C for two days to give small, dark purple crystals. The resulting crystals were combined and washed with DMF (3 × 10 mL) and dried under flowing nitrogen. The chain *cis*-$Mn(Ph_2dhbq)(DMF)_2$ was obtained in 73% yield (108 mg, 0.220 mmol). Anal. Calc. for ($MnC_{24}H_{24}O_6N_2$): C, 58.66; H, 4.92; N, 5.70. Found: C, 58.77; H, 5.04; N, 5.84.

Alternative synthesis of *cis*-Mn(Ph2dhbq)(DMF)2 from Mn^{III}: In a nitrogen-filled glovebox, a solution of H_4Ph_2dhbq (20.0 mg, 0.068 mmol) in DMF (4 mL) was added to a 20 mL scintillation vial. A solution of $Mn(acac)_3$ (24.0 mg, 0.068 mmol, 1 eq.) in DMF (4 mL) was added. The vial was sealed and heated at 80 ˚C for nine days to give a purple powder. The resulting powder was washed with DMF (3 × 10 mL) and dried under flowing nitrogen. The chain *cis*-$Mn(Ph_2dhbq)(DMF)_2$ was obtained in 53% yield (17.5 mg, 0.036 mmol). Anal. Calc. for ($MnC_{24}H_{24}O_6N_2$)(H_2O)$_{0.3}$: C, 58.02; H, 4.99; N, 5.64. Found: C, 57.85; H, 5.02; N, 5.88.

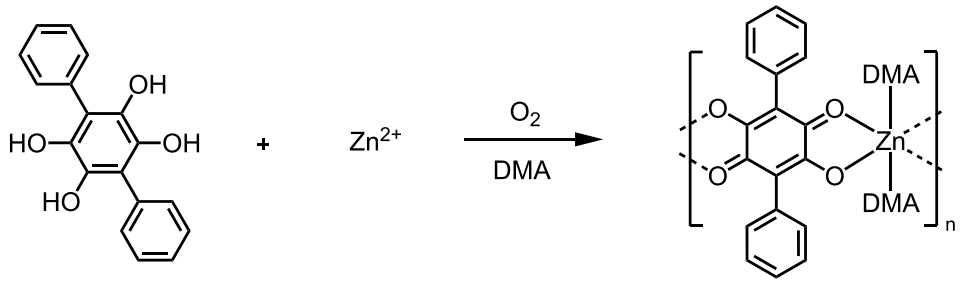

H_4Ph_2dhbq *trans*-$Zn(Ph_2dhbq)(DMA)_2$

Synthesis of *trans*-Zn(Ph$_2$dhbq)(DMA)$_2$: A solution of H_4Ph_2dhbq (89.9 mg, 0.305 mmol) in DMA (30 mL) was divided evenly amongst three 20 mL scintillation vials. A solution of $ZnSO_4 \cdot 6H_2O$ (86.7 mg, 0.311 mmol, 1 eq.) in DMA (30 mL) was added, dividing similarly between the vials. The vials were sealed and heated at 80 ˚C for two days to give a light purple powder. The resulting powder was combined and washed with DMA (3 × 10 mL) and dried under flowing nitrogen. The chain *trans*-$Zn(Ph_2dhbq)(DMA)_2$ was obtained in 61% yield (98.8 mg, 0.186 mmol). Anal. Calc. for $(ZnC_{26}H_{28}O_6N_2)(H_2O)_{1.05}$: C, 56.90; H, 5.53; N, 5.10. Found: C, 56.75; H, 5.12; N, 5.04.

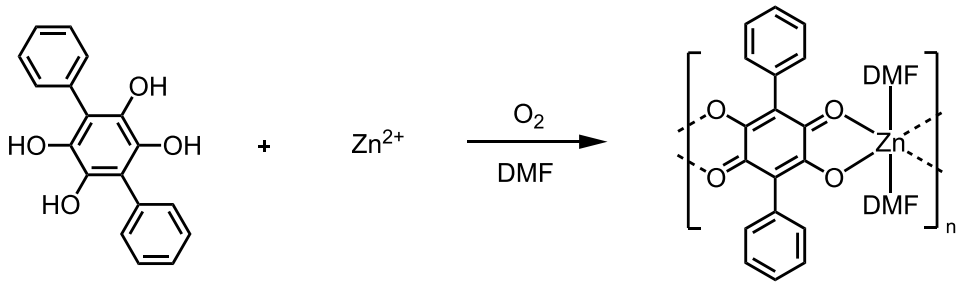

H_4Ph_2dhbq *cis*-$Zn(Ph_2dhbq)(DMF)_2$

Synthesis of *cis*-Zn(Ph$_2$dhbq)(DMF)$_2$: A solution of H_4Ph_2dhbq (86.7 mg, 0.295 mmol) in DMF (30 mL) was divided evenly amongst three 20 mL scintillation vials. A solution of $ZnCl_2$ (40.8 mg, 0.299 mmol, 1 eq.) in MeOH (30 mL) was added, dividing similarly between the vials. The vials were sealed and heated at 80 ˚C for two days to give dark purple crystals. The resulting crystals were combined and washed with DMF (3 × 10 mL) and dried under flowing nitrogen. The chain *cis*-$Zn(Ph_2dhbq)(DMF)_2$ was obtained in 81% yield (119.8 mg, 0.239 mmol). Anal. Calc. for $(ZnC_{24}H_{24}O_6N_2)$: C, 57.44; H, 4.82; N, 5.58. Found: C, 57.38; H, 4.78; N, 5.67.

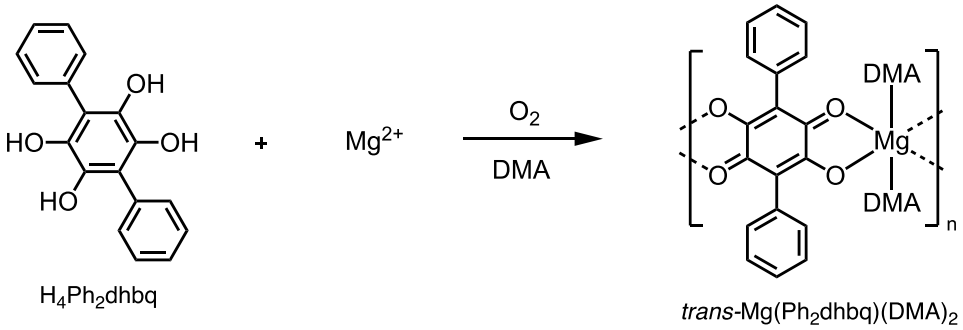

H_4Ph_2dhbq *trans*-$Mg(Ph_2dhbq)(DMA)_2$

Synthesis of *trans*-Mg(Ph₂dhbq)(DMA)₂: A solution of H_4Ph_2dhbq (92.4 mg, 0.314 mmol) in DMA (30 mL) was divided evenly amongst three 20 mL scintillation vials. A solution of $MgSO_4$ (37.3 mg, 0.310 mmol, 1 eq.) in H_2O (30 mL) was added, dividing similarly between the vials. The vials were sealed and heated at 80 ˚C for two days to give a light purple powder. The resulting powder was combined and washed with DMA (3 × 10 mL) and dried under flowing nitrogen. The chain *trans*-$Mg(Ph_2dhbq)(DMA)_2$ was obtained in 72% yield (109.2 mg, 0.223 mmol). Anal. Calc. for $(MgC_{26}H_{28}O_6N_2)(H_2O)_{0.04}$: C, 63.65; H, 5.79; N, 5.71. Found: C, 63.66; H, 5.75; N, 5.69.

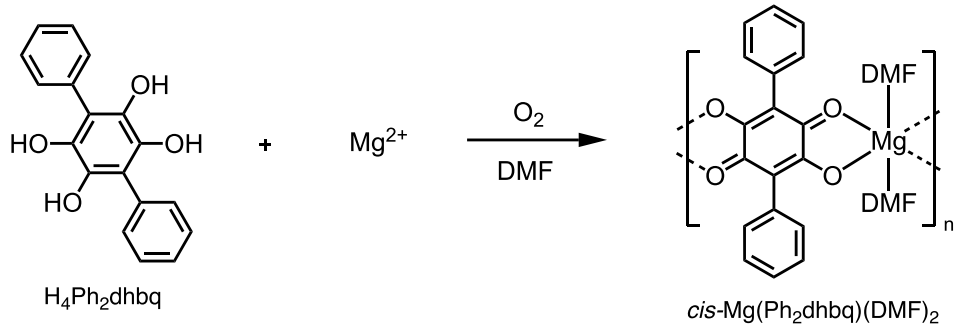

H_4Ph_2dhbq *cis*-$Mg(Ph_2dhbq)(DMF)_2$

Synthesis of *cis*-Mg(Ph₂dhbq)(DMF)₂: A solution of H_4Ph_2dhbq (89.5 mg, 0.304 mmol) in DMF (30 mL) was divided evenly amongst three 20 mL scintillation vials. A solution of $MgCl_2$ (29.6 mg, 0.311 mmol, 1 eq.) in MeOH (30 mL) was added, dividing similarly between the vials. The vials were sealed and heated at 80 ˚C for two days to give small, dark purple crystals. The resulting crystals were combined and washed with DMF (3 × 10 mL) and dried under flowing nitrogen. The chain *cis*-$Mg(Ph_2dhbq)(DMF)_2$ was obtained in 73% yield (102.3 mg, 0.222 mmol). Anal. Calc. for $(MgC_{24}H_{24}O_6N_2)(H_2O)_{0.35}$: C, 61.72; H, 5.33; N, 6.00. Found: C, 61.70; H, 5.23; N, 6.08.

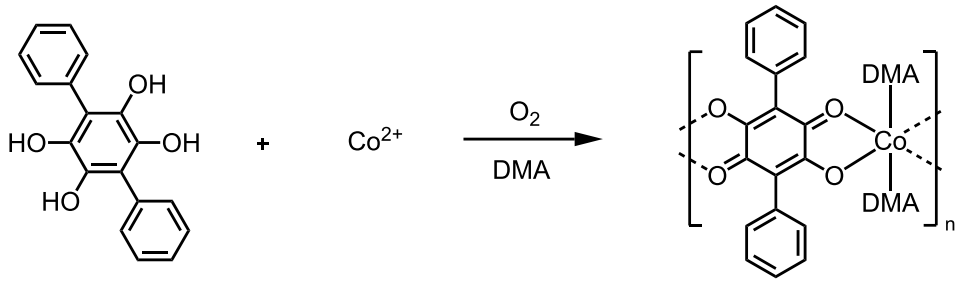

H_4Ph_2dhbq *trans*-$Co(Ph_2dhbq)(DMA)_2$

Synthesis of *trans*-Co(Ph$_2$dhbq)(DMA)$_2$: A solution of H_4Ph_2dhbq (91.1 mg, 0.310 mmol) in DMA (27 mL) was divided evenly amongst three 20 mL culture tubes. A solution of $CoCl_2 \cdot 6H_2O$ (73.3 mg, 0.308 mmol, 1 eq.) in MeOH (27 mL) was carefully layered above the ligand solution, diving similarly between the tubes. The tubes were capped and left undisturbed at room temperature for 14 days to give black crystals. The crystals were combined and washed with DMA (3 × 10 mL) and dried under flowing nitrogen. The chain *trans*-$Co(Ph_2dhbq)(DMA)_2$ was obtained in 62% yield (99.0 mg, 0.189 mmol). Anal. Calc. for $(CoC_{26}H_{28}O_6N_2)(H_2O)_{0.05}(C_4H_9NO)_{0.05}$: C, 59.52; H, 5.44; N, 5.43. Found: C, 59.48; H, 5.42; N, 5.39.

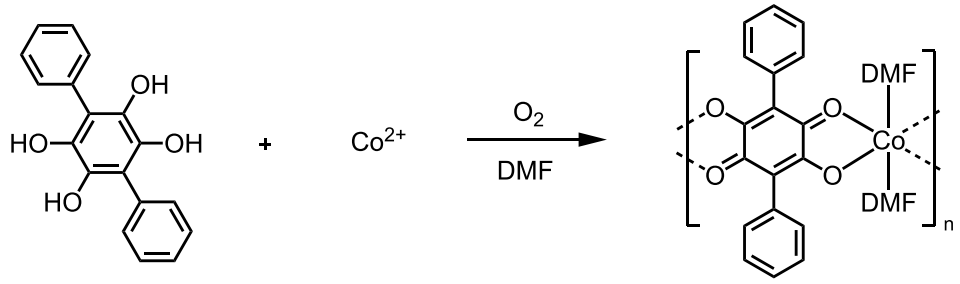

H_4Ph_2dhbq *cis*-$Co(Ph_2dhbq)(DMF)_2$

Synthesis of *cis*-Co(Ph$_2$dhbq)(DMF)$_2$: A solution of H_4Ph_2dhbq (90.1 mg, 0.306 mmol) in DMF (27 mL) was divided evenly amongst three 20 mL culture tubes. A solution of $CoBr_2 \cdot H_2O$ (73.4 mg, 0.310 mmol, 1 eq.) in MeOH (27 mL) was carefully layered above the ligand solution, diving similarly between the tubes. The tubes were capped and left undisturbed at room temperature for 14 days to give a magenta powder. The powders were combined and washed with DMF (3 × 10 mL) and dried under flowing nitrogen. The chain *cis*-$Co(Ph_2dhbq)(DMF)_2$ was obtained in 77% yield (118.6 mg, 0.239 mmol). Anal. Calc. for $(CoC_{24}H_{24}O_6N_2)(H_2O)_{0.3}$: C, 57.56; H, 4.95; N, 5.59. Found: C, 57.46; H, 4.86; N, 5.54.

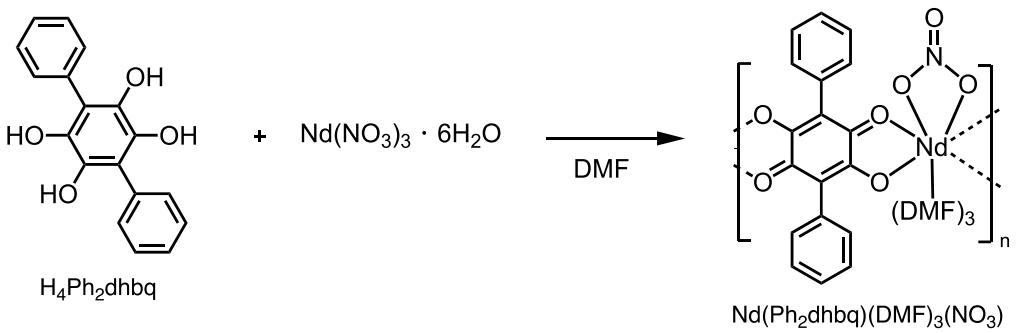

H_4Ph_2dhbq $Nd(Ph_2dhbq)(DMF)_3(NO_3)$

Synthesis of $Nd(Ph_2dhbq)(DMF)_3(NO_3)$ for SCXRD: In a nitrogen-filled glovebox, a solution of H_4Ph_2dhbq (2.5 mg, 0.0085 mmol) in DMF (1 mL) was added to a 4 mL scintillation vial. A solution of $Nd(NO_3)_3{\cdot}6H_2O$ (3.8 mg, 0.0085 mmol, 1.0 eq.) in DMF (1 mL) was layered above the solution of H_4Ph_2dhbq. The vial was sealed and heated at 120 ˚C for 3 days to give small, dark purple block-shaped crystals suitable for X-ray diffraction.

Synthesis of $Nd(Ph_2dhbq)(DMF)_3(NO_3)$: In a nitrogen-filled glovebox, a solution of H_4Ph_2dhbq (68.2 mg, 0.232 mmol) in DMF (6 mL) was divided equally between two 20 mL scintillation vial. A solution of $Nd(NO_3)_3{\cdot}6H_2O$ (103 mg, 0.234 mmol, 1 eq.) in DMF (6 mL) was divided similarly between the two vials. The vials were sealed and heated at 120 ˚C for two weeks to give small dark purple crystals. The crystals were combined, washed with DMF (3 × 20 mL), and dried under flowing nitrogen. The chain $Nd(Ph_2dhbq)(DMF)_3(NO_3)$ was obtained in 36% yield (59.1 mg, 0.0826 mmol). Anal. Calc. for $(NdC_{27}H_{31}O_{10}N_4)(H_2O)_{0.2}$: C, 45.08; H, 4.40; N, 7.79. Found: C, 45.03; H, 4.31; N, 7.76.

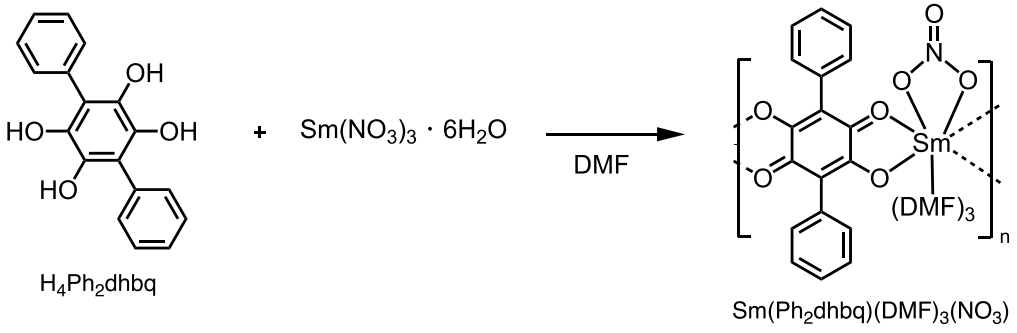

H_4Ph_2dhbq $Sm(Ph_2dhbq)(DMF)_3(NO_3)$

Synthesis of $Sm(Ph_2dhbq)(DMF)_3(NO_3)$: In a nitrogen-filled glovebox, a solution of H_4Ph_2dhbq (19.9 mg, 0.068 mmol) in DMF (4 mL) was added to a 20 mL scintillation vial. A solution of $Sm(NO_3)_3{\cdot}6H_2O$ (30.0 mg, 0.067 mmol, 1 eq.) in DMF (4 mL) was added. The vial was sealed and heated at 120 ˚C for seven days to give small dark crystals. The resulting crystals were washed with DMF at 80 ˚C (3 × 10 mL) and dried under flowing nitrogen. The chain $Sm(Ph_2dhbq)(DMF)_3(NO_3)$ was obtained in 13% yield (6.2 mg, 0.0086 mmol). Anal. Calc. for $(SmC_{27}H_{31}O_{10}N_4)(H_2O)_{0.5}(C_3H_7NO)_{0.1}$: C, 44.41; H, 4.46; N, 7.78. Found: C, 44.43; H, 4.38; N, 7.86.

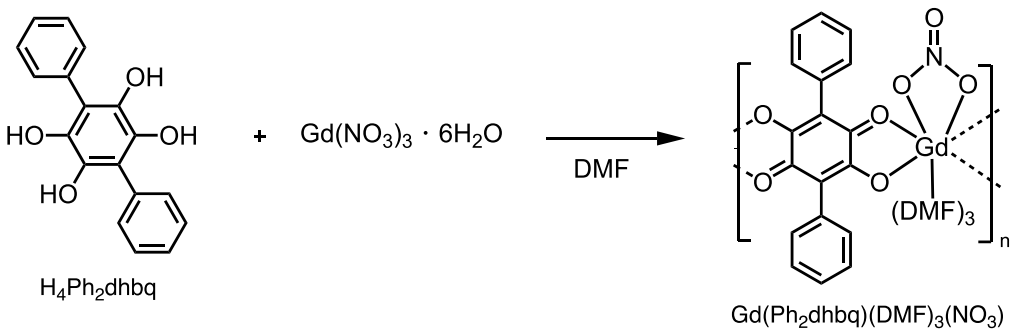

H_4Ph_2dhbq $Gd(Ph_2dhbq)(DMF)_3(NO_3)$

Synthesis of $Gd(Ph_2dhbq)(DMF)_3(NO_3)$: In a nitrogen-filled glovebox, a solution of H_4Ph_2dhbq (20.0 mg, 0.068 mmol) in DMF (4 mL) was added to a 20 mL scintillation vial. A solution of $Gd(NO_3)_3{\cdot}6H_2O$ (30.7 mg, 0.067 mmol, 1 eq.) in DMF (4 mL) was added. The vial was sealed and heated at 120 ˚C for seven days to give small dark crystals. The resulting crystals were washed with DMF at 80 ˚C (3 × 10 mL) and dried under flowing nitrogen. The chain $Gd(Ph_2dhbq)(DMF)_3(NO_3)$ was obtained in 16% yield (7.7 mg, 0.0094 mmol). Anal. Calc. for ($GdC_{27}H_{31}O_{10}N_4$): C, 44.49; H, 4.29; N, 7.69. Found: C, 48.27; H, 4.15; N, 5.69.

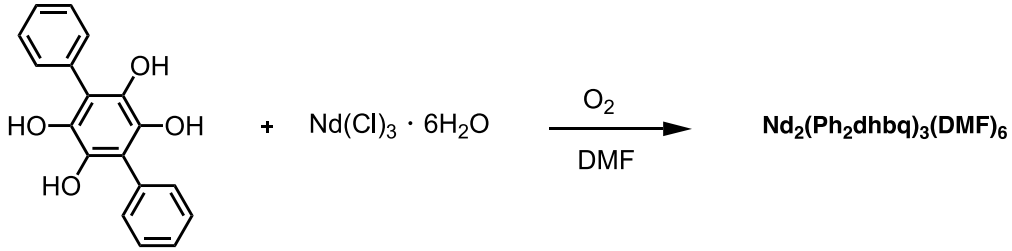

H_4Ph_2dhbq

Synthesis of $Nd_2(Ph_2dhbq)_3(DMF)_6$ for SCXRD: In a nitrogen-filled glovebox, a solution of H_4Ph_2dhbq (5.0 mg, 0.017 mmol) in DMF (1 mL) was added to a 4 mL scintillation vial. A solution of $NdCl_3{\cdot}\ 6H_2O$ (4.2 mg, 0.017 mmol, 1 eq.) in DMF (1 mL) was layered above the solution of H_4Ph_2dhbq. The vial was removed from the glovebox, opened to air, then sealed and heated at 120 ˚C to give small, dark purple block-shaped crystals suitable for X-ray diffraction.

Synthesis of $Nd_2(Ph_2dhbq)_3(DMF)_6$: In a nitrogen-filled glovebox, a solution of H_4Ph_2dhbq (20.0 mg, 0.068 mmol) in DMF (4 mL) was added to a 20 mL scintillation vial followed by a solution of $NdCl_3{\cdot}\ 6H_2O$ (17.0 mg, 0.067 mmol, 1 eq.) in DMF (4 mL). The vial was removed from the box, opened to air, then sealed and heated at 120 ˚C for five days to give small purple crystals. The crystals were washed with DMF at 80 ˚C (3 × 10 mL) and dried under flowing nitrogen. The 2D network $Nd_2(Ph_2dhbq)_3(DMF)_6$ was obtained in 7% yield (4.7 mg, 0.0025 mmol). Anal. Calc. for ($Nd_2C_{54}H_{30}O_{12}[C_3H_7NO]_{5.1}[H_2O]_{0.9})(H_2O)_{1.4}$: C, 52.90; H, 4.50; N, 4.54. Found: C, 52.72; H, 4.26; N, 4.77.

Note: best fit for combustion analysis data suggests that a small amount of coordinated DMF (less than one molecule per formula unit) may be replaced by H_2O in this structure.

3. Single Crystal X-ray Diffraction:

Standard single-crystal X-ray diffraction (SCXRD) data were collected on a Bruker APEX II single crystal X-ray diffractometer equipped with a Mo-radiation source and a Miracol X-ray optical collimator. Synchrotron SCXRD data were collected on Beamline 12.2.1 at the Advanced Light Source (ALS), Lawrence Berkeley National Lab (Berkeley, CA, USA).

The data was integrated and scaled using SAINT, SADABS within the APEX2 software package by Bruker.[2] Solution by direct methods using SHELXT produced complete heavy atom phasing models consistent with the proposed structures.[3,4] The structures were completed by difference Fourier synthesis with SHELXL.[5,6] Scattering factors are from Waasmair and Kirfel.[7] Hydrogen atoms were placed in geometrically idealized positions and constrained to ride on their parent atoms with C–H distances in the range 0.95-1.00 Å. Isotropic thermal parameters U_{eq} were fixed such that they were $1.2U_{eq}$ of their parent atom U_{eq} for CH's and $1.5U_{eq}$ of their parent atom U_{eq} for methyl groups. All non-hydrogen atoms were refined anisotropically by full-matrix least-squares.

SCXRD of *trans*-Mn(Ph$_2$dhbq)(DMA)$_2$: A purple needle measuring 0.13 × 0.04 × 0.04 mm^3 was mounted on a loop with oil. Data was collected at 100 K. Crystal-to-detector distance was 40 mm and exposure time was 60 seconds per frame for all sets. The scan width was 0.5˚. Data collection was 100% complete to 25˚ in θ. A total of 9415 merged reflections were collected covering the indices: $-10 \leq h \leq 10$, $-17 \leq k \leq 14$, $-15 \leq l \leq 15$. 3018 reflections were symmetry independent with $R_{int} = 0.0936$. Indexing and unit cell refinement indicated a primitive monoclinic lattice. The space group was found to be P $2_1/c$ (No. 14).

The displacement parameters of the disordered DMF were stabilized via EADP (C10/C10B) and ISOR (C10, C11/C11B). The geometries of the two disordered DMF were linked with a 'SAME' command.

SCXRD of *cis*-Mn(Ph$_2$dhbq)(DMF)$_2$: Data were collected using a synchrotron X-ray source. A purple needle measuring 0.12 × 0.02 × 0.02 mm^3 was mounted on a loop with oil. Data was collected at 100 K. Data collection was 100% complete to 25˚ in θ. A total of 31856 merged reflections were collected covering the indices: $-12 \leq h \leq 12$, $-12 \leq k \leq 12$, $-23 \leq l \leq 23$. 4271 reflections were symmetry independent with $R_{int} = 0.0716$. Indexing and unit cell refinement indicated a primitive trigonal lattice. The space group was found to be P 3_1 (No. 144).

The racemate (chiral space group P3(1)) required a TWIN card (1 0 0 –1 –1 0 0 0 1) and BASF refinement (BASF = 0.497(4)) . Phenyl groups were optimized via AFIX 66 … AFIX 0 loops.

SCXRD of Nd(Ph$_2$dhbq)(DMF)$_3$(NO$_3$): A purple prism measuring 0.14 × 0.07 × 0.03 mm^3 was mounted on a loop with oil. Data was collected at 100 K. Crystal-to-detector distance was 40 mm and exposure time was 15 seconds per frame for all sets. The scan width was 0.5˚. Data collection was 100% complete to 25˚ in θ. A total of 11769 reflections were collected covering the indices,

$-16 \leq h \leq 16$, $-18 \leq k \leq 18$, $-19 \leq l \leq 19$. 11769 reflections were symmetry independent and the $R_{int} = 0.0496$. Indexing and unit cell refinement indicated a triclinic lattice. The space group was found to be P $\bar{1}$ (No. 2).

The displacement parameters of a few atoms (N4 O8 O9 N2 C24) were linked along bonds via a DELU card and those of C24/C24 in addition stabilized with an ISOR command and the disordered C24/C24 was set to share equal displacement via 'EADP'.

SCXRD of $Nd_2(Ph_2dhbq)_3(DMF)_6$: Data were collected using a synchrotron X-ray source. A purple plate measuring $0.07 \times 0.05 \times 0.02$ mm^3 was mounted on a loop with oil. Data was collected at 100 K. Crystal-to-detector distance was 47.1 mm and exposure time was 1 second per frame for all sets. The scan width was 0.5˚. Data collection was 91.4% complete to 25˚ in θ. A total of 57327 reflections were collected covering the indices, $-12 \leq h \leq 12$, $-12 \leq k \leq 12$, $-22 \leq l \leq 22$. 16406 reflections were symmetry independent and the $R_{int} = 0.0836$. Indexing and unit cell refinement indicated a triclinic lattice. The space group was found to be P $\bar{1}$ (No. 2).

Two disordered DMF solvent molecules required planarization ('FLAT' commands) and linking of displacement parameters ('SIMU' card) due to partial overlap of the atoms. In addition, the geometries of all DMF solvents are linked to a better defined 'template' DMF, (O13 ... C57). The water hydrogen atoms were 'attached' to the oxygen with DFIX restraints, and 5 isolated carbons and two oxygen atoms needed 'ISOR' stabilization.

Table S1. Crystallographic data for *trans*-Mn(Ph$_2$dhbq)(DMA)$_2$.

Empirical formula	C26 H28 Mn N2 O6	
Formula weight	519.44	
Temperature	100(2) K	
Wavelength	0.71073 Å	
Crystal system	Monoclinic	
Space group	P 2_1/c	
Unit cell dimensions	a = 8.0608(9) Å	α = 90˚
	b = 13.3977(14) Å	β = 91.241(6)˚
	c = 11.7569(14) Å	γ = 90˚
Volume	1269.4(2) Å^3	
Z	2	
Density (calculated)	1.359 Mg/m^3	
Absorption coefficient	0.563 mm^{-1}	
F(000)	542	
Crystal size	0.130 × 0.040 × 0.040 mm^3	
Theta range for data collection	2.305 to 27.853˚	
Index ranges	$-10 \le h \le 10$, $-17 \le k \le 14$, $-15 \le l \le 15$	
Reflections collected	9415	
Independent reflections	3018 [R_{int} = 0.0936]	
Completeness to theta = 25.000˚	100.0%	
Refinement method	Full-matrix least-squares on F^2	
Data / restraints / parameters	3018 / 26 / 215	
Goodness-of-fit on F^2	0.976	
Final R indices [I>2sigma(I)]	R1 = 0.0479, wR2 = 0.0963	
R indices (all data)	R1 = 0.1057, wR2 = 0.1153	
Largest diff. peak and hole	0.306 and –0.456 e Å^{-3}	

Table S2. Crystallographic data for *cis*-Mn(Ph$_2$dhbq)(DMF)$_2$.

Empirical formula	C24 H24 Mn N2 O6	
Formula weight	491.39	
Temperature	100(2) K	
Wavelength	0.7288 Å	
Crystal system	Trigonal	
Space group	P 3_1	
Unit cell dimensions	a = 10.1118(12) Å	α = 90˚
	b = 10.1118(12) Å	β = 90˚
	c = 18.832(3) Å	γ = 120˚
Volume	1667.6(5) Å^3	
Z	3	
Density (calculated)	1.468 Mg/m^3	
Absorption coefficient	0.677 mm^{-1}	
F(000)	765	
Crystal size	0.120 × 0.020 × 0.020 mm^3	
Theta range for data collection	2.218 to 26.831˚	
Index ranges	$-12 \le h \le 12$, $-12 \le k \le 12$, $-23 \le l \le 23$	
Reflections collected	31856	
Independent reflections	4271 [R_{int} = 0.0716]	
Completeness to theta = 25.930˚	100.0%	
Absorption correction	Semi-empirical from equivalents	
Max. and min. transmission	0.9453 and 0.8080	
Refinement method	Full-matrix least-squares on F^2	
Data / restraints / parameters	4271 / 1 / 279	
Goodness-of-fit on F^2	1.073	
Final R indices [I>2sigma(I)]	R1 = 0.0374, wR2 = 0.0982	
R indices (all data)	R1 = 0.0403, wR2 = 0.1001	
Absolute structure parameter	0.497(4)	
Largest diff. peak and hole	0.341 and –0.297 e A^{-3}	

Table S3: Crystallographic data for $Nd(Ph_2dhbq)(DMF)_3(NO_3)$.

Empirical formula	C27 H31 N4 Nd O10	
Formula weight	715.80	
Temperature	100(2) K	
Wavelength	0.71073 Å	
Crystal system	Triclinic	
Space group	P -1	
Unit cell dimensions	a = 10.4589(17) Å	α = 93.854(8)˚
	b = 12.0484(19) Å	β = 113.574(8)˚
	c = 12.740(2) Å	γ = 91.387(8)˚
Volume	1465.8(4) $Å^3$	
Z	2	
Density (calculated)	1.622 Mg/m^3	
Absorption coefficient	1.833 mm^{-1}	
F(000)	722	
Crystal size	0.140 × 0.070 × 0.030 mm^3	
Theta range for data collection	1.697 to 33.805˚	
Index ranges	$-16 \le h \le 16$, $-18 \le k \le 18$, $-19 \le l \le 19$	
Reflections collected	84305	
Independent reflections	11769 [R_{int} = 0.0496]	
Completeness to theta = 25.242˚	100.0%	
Refinement method	Full-matrix least-squares on F^2	
Data / restraints / parameters	11769 / 11 / 390	
Goodness-of-fit on F^2	1.046	
Final R indices [I>2sigma(I)]	R1 = 0.0190, wR2 = 0.0448	
R indices (all data)	R1 = 0.0213, wR2 = 0.0457	
Largest diff. peak and hole	1.207 and –0.789 e $Å^{-3}$	

Table S4: Crystallographic data for $Nd_2(Ph_2dhbq)_3(DMF)_6$.

Empirical formula	C84 H102 N10 Nd2 O23	
Formula weight	1908.23	
Temperature	100(2) K	
Wavelength	0.7288 Å	
Crystal system	Triclinic	
Space group	P -1	
Unit cell dimensions	a = 12.033(6) Å	α = 81.48(2)˚
	b = 14.668(7) Å	β = 88.19(2)˚
	c = 27.099(12) Å	γ = 69.49(2)˚
Volume	4429(4) $Å^3$	
Z	2	
Density (calculated)	1.431 Mg/m^3	
Absorption coefficient	1.311 mm^{-1}	
F(000)	1960	
Crystal size	0.070 × 0.050 × 0.020 mm^3	
Theta range for data collection	0.779 to 27.097˚	
Index ranges	$-12 \le h \le 12$, $-12 \le k \le 12$, $-22 \le l \le 22$	
Reflections collected	57327	
Independent reflections	16406 [R_{int} = 0.0836]	
Completeness to theta = 25.930˚	91.4%	
Refinement method	Full-matrix least-squares on F^2	
Data / restraints / parameters	16406 / 835 / 1171	
Goodness-of-fit on F^2	0.977	
Final R indices [I>2sigma(I)]	R1 = 0.0903, wR2 = 0.2262	
R indices (all data)	R1 = 0.1301, wR2 = 0.2547	
Extinction coefficient	0.0014(3)	
Largest diff. peak and hole	2.188 and –2.623 e $Å^{-3}$	

4. Powder X-ray Diffraction

Powder X-ray diffraction (PXRD) data were collected on a Bruker D2 PHASER benchtop diffractometer equipped with a LINXEYE XE-T detector. Samples were ground with a spatula and analyzed as dry powders on a monocrystalline Si substrate.

Data analysis was performed in the TOPAS software package by Bruker. Indexing and Pawley refinement of all structures were successfully performed using the space groups determined from the SCXRD structures of the corresponding isostructural Mn or Nd chains. Refinement was performed using Pseudo-Voigt functions for all data.

Table S5: Unit cell parameters determined from the Pawley refinement of the PXRD patterns of *trans*-M(Ph_2dhbq)$(DMA)_2$ (M = Zn, Mg, and Co) in the space group $P2_1/c$ (No. 14), relative to the SCXRD structure of *trans*-Mn(Ph_2dhbq)$(DMA)_2$.

chain	**a** (Å)	**b** (Å)	**c** (Å)	**α** (˚)	**β** (˚)	**γ** (˚)	R_{Bragg}
trans-Mn	8.0608(9)	13.3977(14)	11.7569(14)	90	91.241(6)	90	-
trans-Zn	7.8476(13)	13.509(2)	11.9729(19)	90	90.44(4)	90	1.9
trans-Mg	7.846(3)	13.510(5)	11.979(4)	90	90.29(6)	90	0.8
trans-Co	10.833(17)	13.434(11)	12.278(8)	90	80.94(6)	90	1.8

Table S6: Unit cell parameters determined from the Pawley refinement of the PXRD patterns of *cis*-M(Ph_2dhbq)$(DMF)_2$ (M = Zn, Mg, and Co) in the space group $P3_1$ (No. 144), relative to the SCXRD structure of *cis*-Mn(Ph_2dhbq)$(DMF)_2$.

chain	**a** (Å)	**b** (Å)	**c** (Å)	**α** (˚)	**β** (˚)	**γ** (˚)	R_{Bragg}
cis-Mn	10.1118(12)	10.1118(12)	18.832(3)	90	90	120	-
cis-Zn	10.2632(14)	10.2632(14)	19.016(4)	90	90	120	1.2
cis-Mg	10.3078(12)	10.3078(12)	18.983(3)	90	90	120	2.3
cis-Co	10.272(4)	10.272(4)	19.030(8)	90	90	120	0.2

Table S7: Unit cell parameters determined from the Pawley refinement of the PXRD patterns of $M(Ph_2dhbq)(DMF)_3(NO_3)$ (M = Sm and Gd) in the space group P-1 (No. 2), relative to the SCXRD structure of $Nd(Ph_2dhbq)(DMF)_3(NO_3)$.

chain	**a** (Å)	**b** (Å)	**c** (Å)	**α** (˚)	**β** (˚)	**γ** (˚)	$\mathbf{R_{Bragg}}$
Nd	10.4589(17)	12.0484(19)	12.740(2)	93.854(8)	113.574(8)	91.387(8)	-
Sm	10.81(2)	12.35(2)	13.09(3)	85.29(10)	115.50(15)	89.34(14)	3.8
Gd	10.479(9)	12.049(9)	12.612(13)	94.17(6)	112.06(6)	91.74(6)	1.3

5. Supplementary Figures

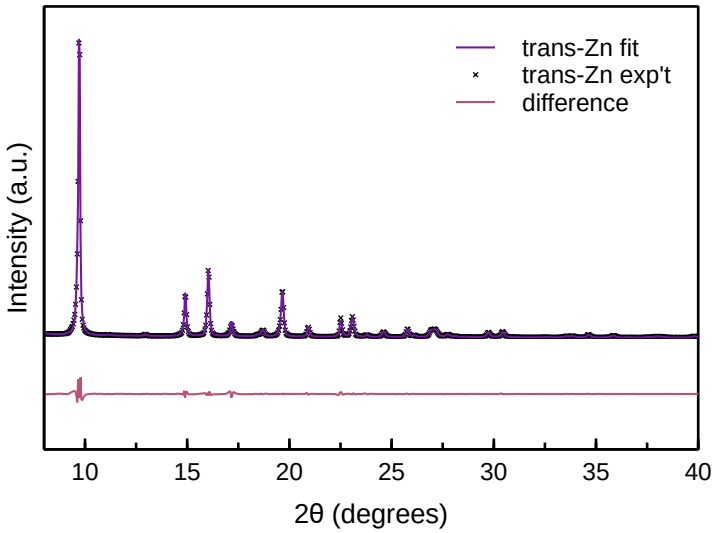

Figure S1. Pawley refinement of the PXRD pattern of *trans*-Zn(Ph$_2$dhbq)(DMA)$_2$. Experimental data (black ×'s) are shown in comparison to the calculated fit (upper solid trace, purple) and difference plot (lower solid trace, pink).

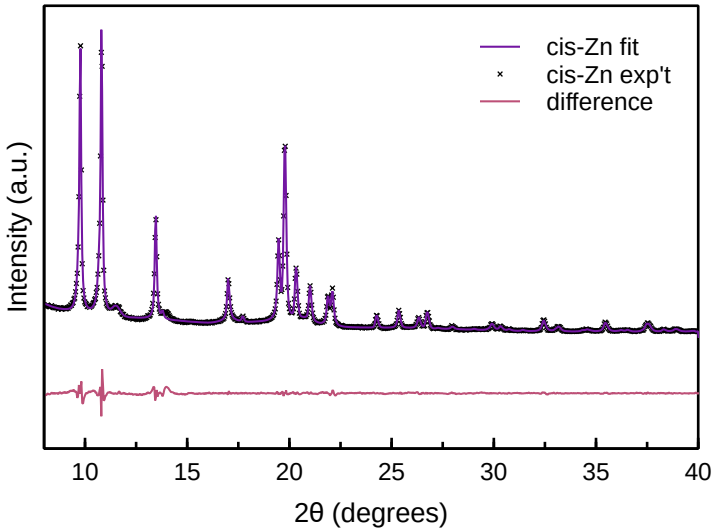

Figure S2. Pawley refinement of the PXRD pattern of *cis*-Zn(Ph$_2$dhbq)(DMF)$_2$. Experimental data (black ×'s) are shown in comparison to the calculated fit (upper solid trace, purple) and difference plot (lower solid trace, pink).

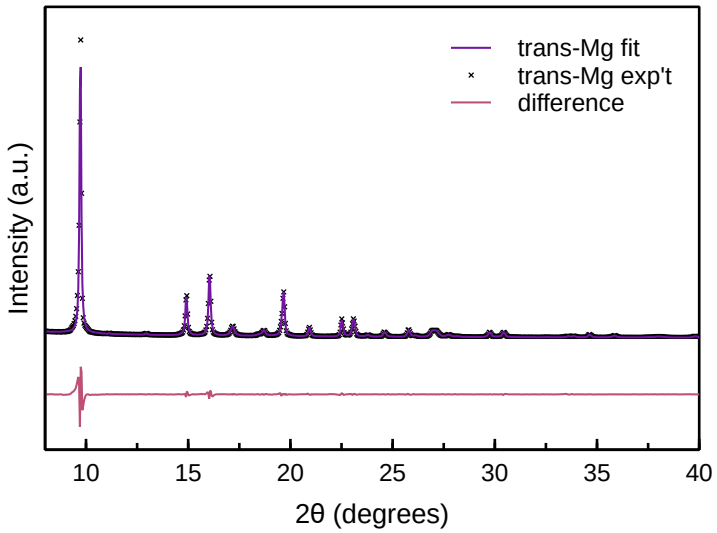

Figure S3. Pawley refinement of the PXRD pattern of *trans*-Mg(Ph$_2$dhbq)(DMA)$_2$. Experimental data (black ×'s) are shown in comparison to the calculated fit (upper solid trace, purple) and difference plot (lower solid trace, pink).

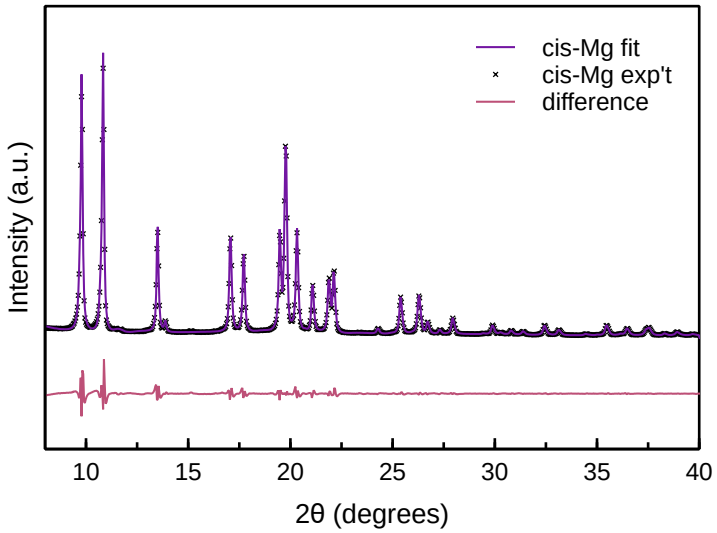

Figure S4. Pawley refinement of the PXRD pattern of *cis*-Mg(Ph$_2$dhbq)(DMF)$_2$. Experimental data (black ×'s) are shown in comparison to the calculated fit (upper solid trace, purple) and difference plot (lower solid trace, pink).

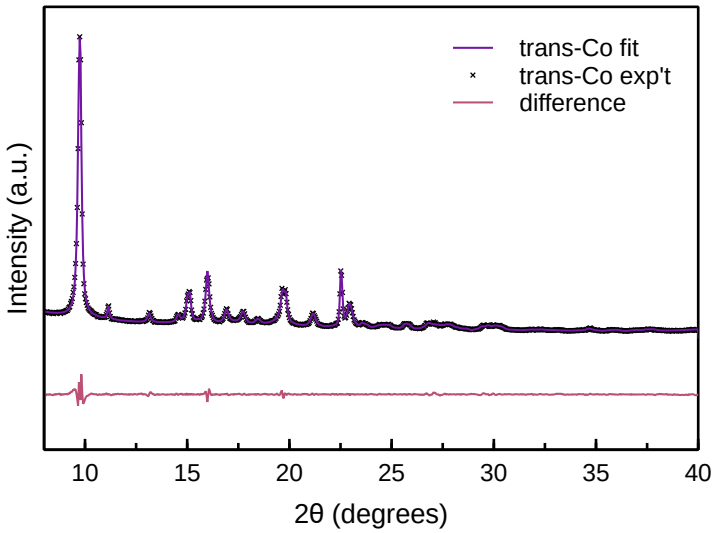

Figure S5. Pawley refinement of the PXRD pattern of *trans*-Co(Ph$_2$dhbq)(DMA)$_2$. Experimental data (black ×'s) are shown in comparison to the calculated fit (upper solid trace, purple) and difference plot (lower solid trace, pink).

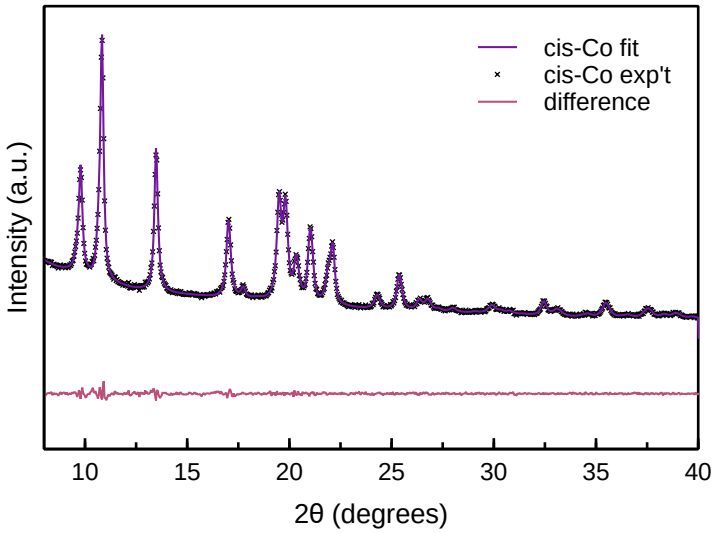

Figure S6. Pawley refinement of the PXRD pattern of *cis*-Co(Ph$_2$dhbq)(DMF)$_2$. Experimental data (black ×'s) are shown in comparison to the calculated fit (upper solid trace, purple) and difference plot (lower solid trace, pink).

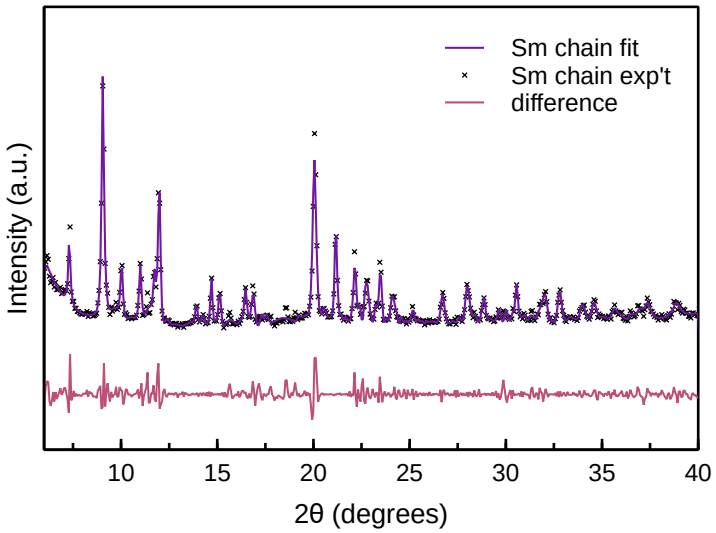

Figure S7. Pawley refinement of the PXRD pattern of $Sm(Ph_2dhbq)(DMF)_3(NO_3)$. Experimental data (black ×'s) are shown in comparison to the calculated fit (upper solid trace, purple) and difference plot (lower solid trace, pink).

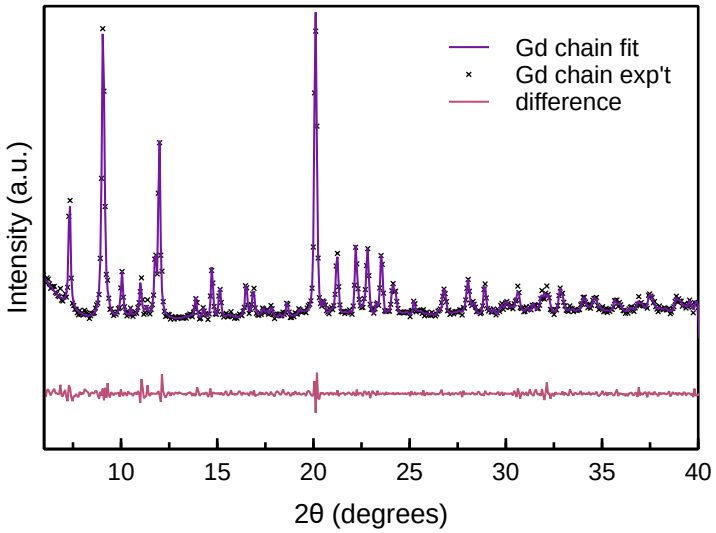

Figure S8. Pawley refinement of the PXRD pattern of $Gd(Ph_2dhbq)(DMF)_3(NO_3)$. Experimental data (black ×'s) are shown in comparison to the calculated fit (upper solid trace, purple) and difference plot (lower solid trace, pink).

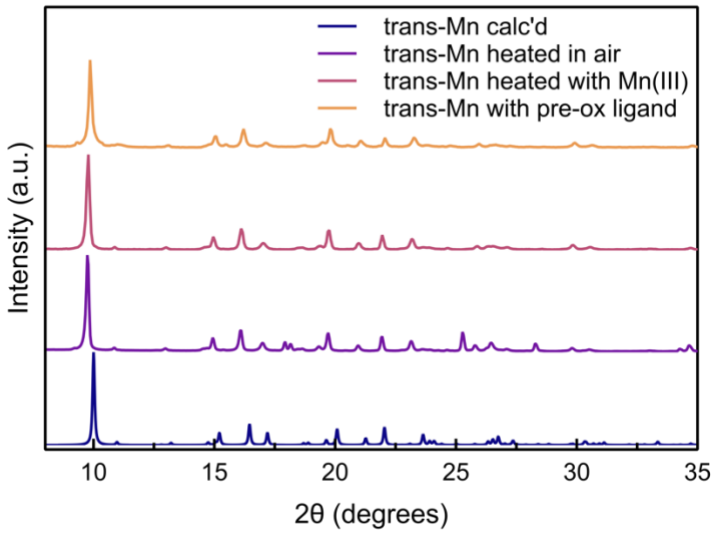

Figure S9. Experimental PXRD patterns of *trans*-Mn(Ph_2dhbq)($DMA)_2$ synthesized from (top to bottom) oxidized H_2Ph_2dhbq with Mn^{II} with heat under an inert atmosphere, reduced H_4Ph_2dhbq with Mn^{III} with heat under an inert atmosphere, and reduced H_4Ph_2dhbq with Mn^{II} with heat in air, compared to the calculated PXRD of *trans*-Mn(Ph_2dhbq)($DMA)_2$.

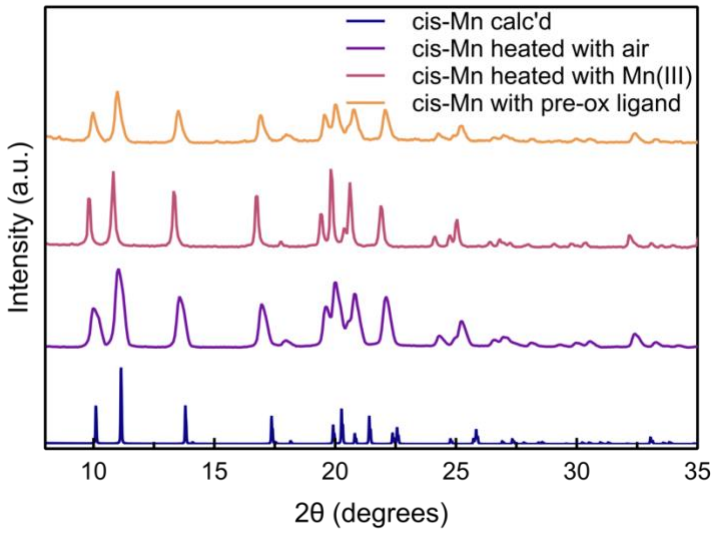

Figure S10. Experimental PXRD patterns of *cis*-Mn(Ph_2dhbq)($DMF)_2$ synthesized from (top to bottom) oxidized H_2Ph_2dhbq with Mn^{II} with heat under an inert atmosphere, reduced H_4Ph_2dhbq with Mn^{III} with heat under an inert atmosphere, and reduced H_4Ph_2dhbq with Mn^{II} with heat in air, compared to the calculated PXRD of *cis*-Mn(Ph_2dhbq)($DMF)_2$.

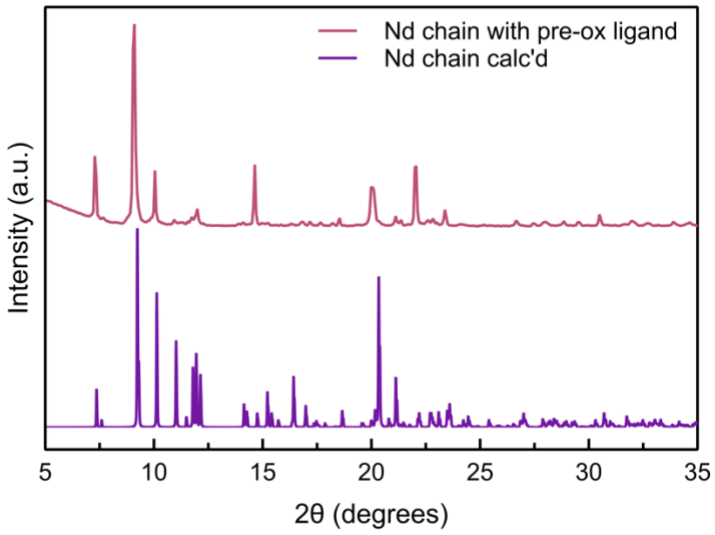

Figure S11. Preliminary experimental PXRD pattern of (top) $Nd(Ph_2dhbq)(DMF)_3(NO_3)$ synthesized from neodymium(III) nitrate with the oxidized H_2Ph_2dhbq under an inert atmosphere compared to (bottom) the calculated PXRD pattern $Nd(Ph_2dhbq)(DMF)_3(NO_3)$.

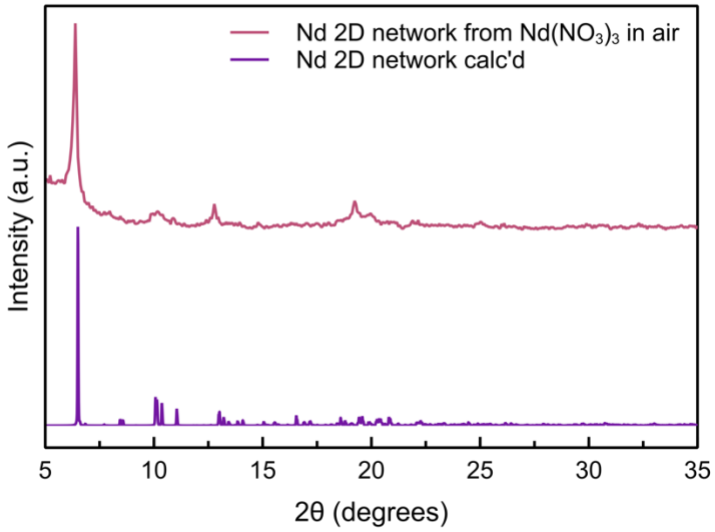

Figure S12. Preliminary experimental PXRD pattern of (top) $Nd_2(Ph_2dhbq)_3(DMF)_6$ synthesized from neodymium(III) nitrate in air compared to (bottom) the calculated PXRD pattern of $Nd_2(Ph_2dhbq)_3(DMF)_6$.

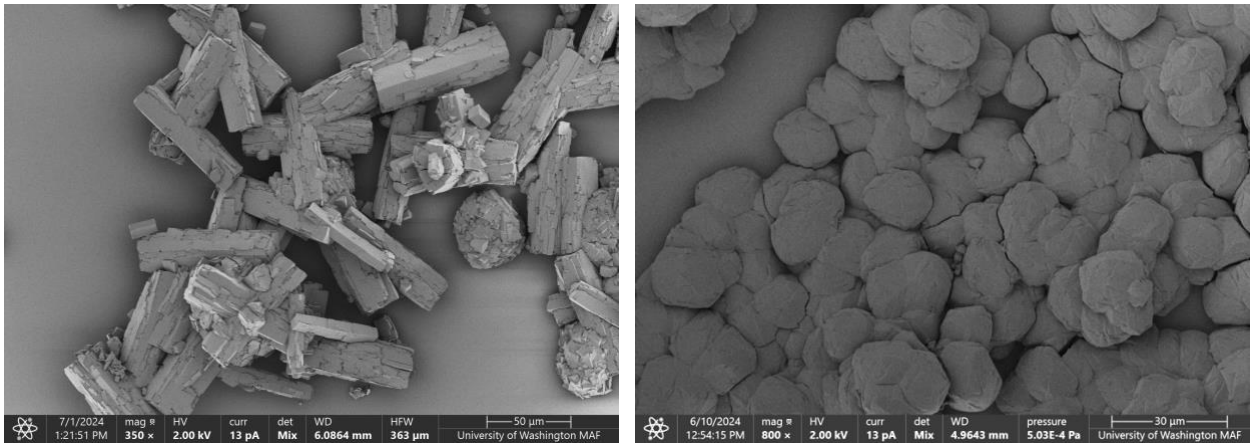

Figure S13. SEM images of (left) *trans*-Mn(Ph$_2$dhbq)(DMA)$_2$ and (right) *cis*-Mn(Ph$_2$dhbq)(DMF)$_2$ synthesized from the oxidized H$_2$Ph$_2$dhbq with Mn^{II} in DMA or DMF with heat under an inert atmosphere.

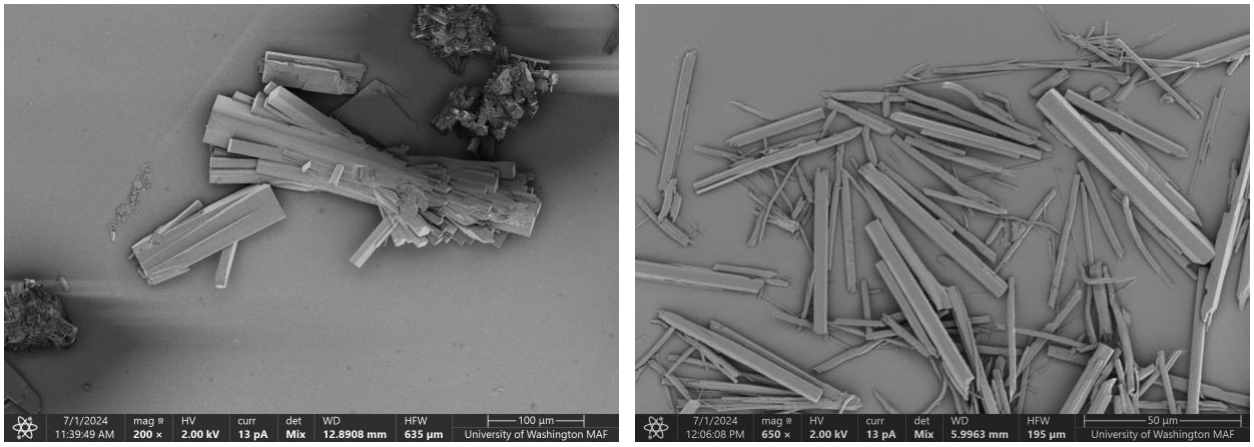

Figure S14. SEM images of (left) *trans*-Mn(Ph$_2$dhbq)(DMA)$_2$ and (right) *cis*-Mn(Ph$_2$dhbq)(DMF)$_2$ synthesized from the reduced H$_4$Ph$_2$dhbq with Mn^{II} in layered MeOH/DMA or MeOH/DMF at room temperature in air.

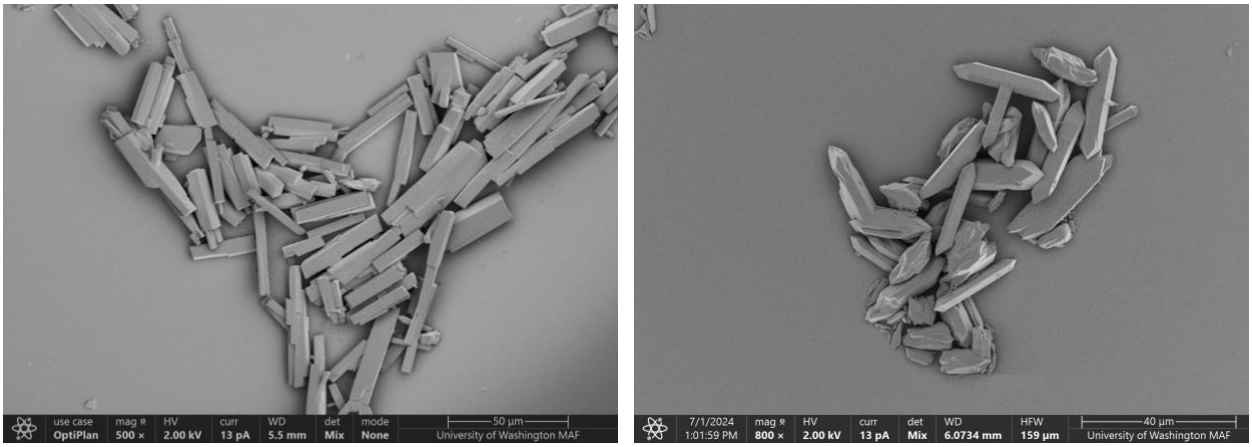

Figure S15. SEM images of (left) *trans*-Mn(Ph$_2$dhbq)(DMA)$_2$ and (right) *cis*-Mn(Ph$_2$dhbq)(DMF)$_2$ synthesized from the reduced H$_4$Ph$_2$dhbq with Mn^{II} in DMA or DMF with heat in air.

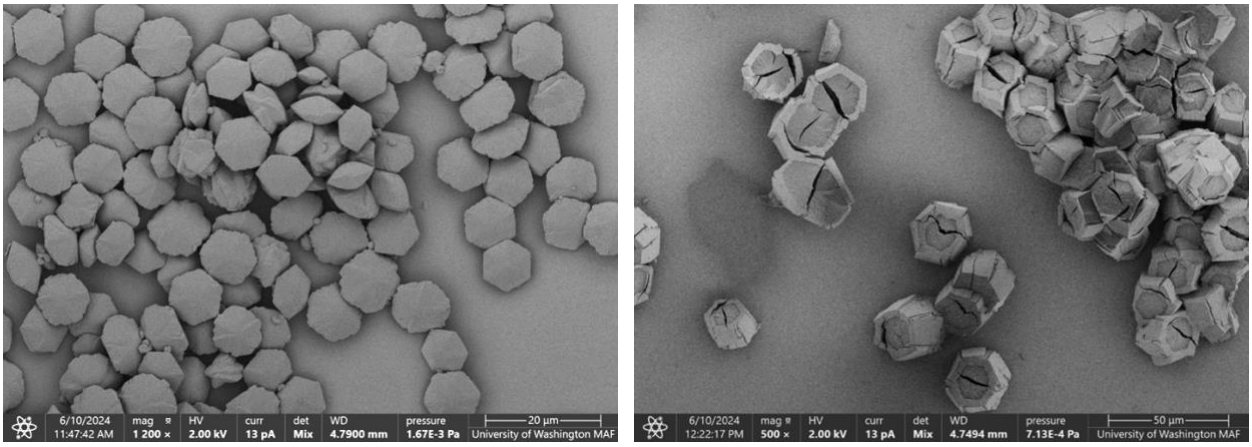

Figure S16. SEM images of (left) *trans*-Mn(Ph$_2$dhbq)(DMA)$_2$ and (right) *cis*-Mn(Ph$_2$dhbq)(DMF)$_2$ synthesized from the reduced H$_4$Ph$_2$dhbq with Mn^{III} in DMA or DMF with heat under an inert atmosphere.

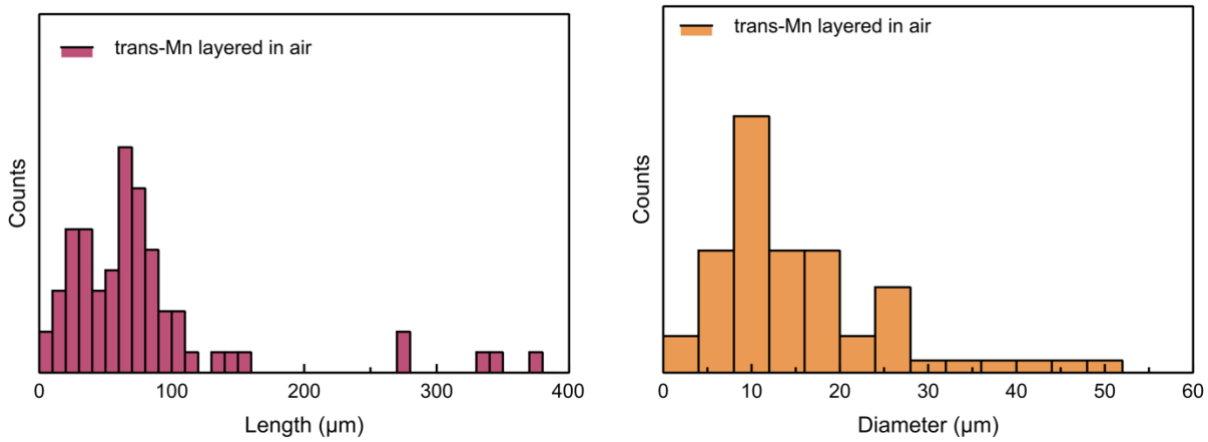

Figure S17. Particle size distributions derived from the SEM images of *trans*-Mn(Ph$_2$dhbq)(DMA)$_2$ synthesized from the reduced H$_4$Ph$_2$dhbq with Mn^{II} in layered MeOH/DMA at room temperature in air. The average particle length is 80.3 ± 70.2 μm and diameter is 15.4 ± 10.0 μm.

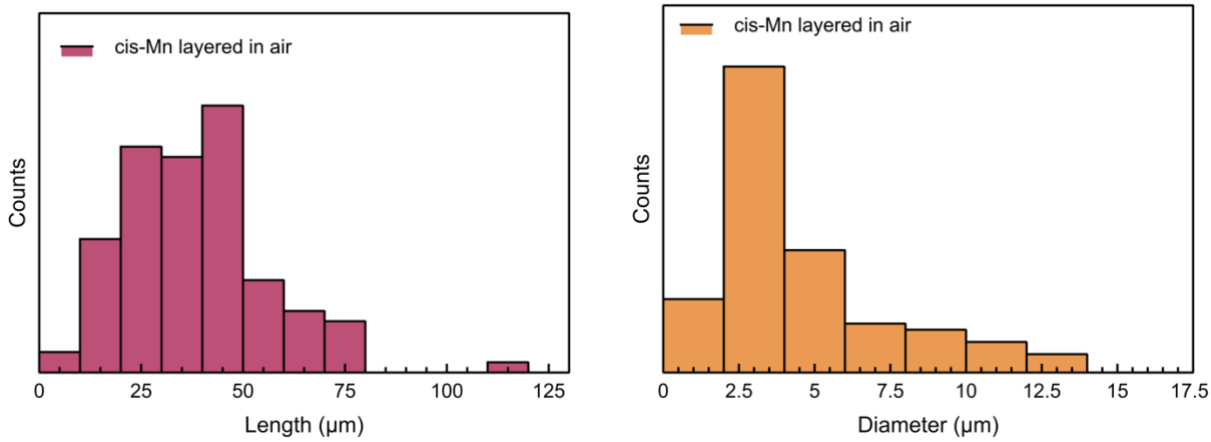

Figure S18. Particle size distributions derived from the SEM images of *cis*-Mn(Ph$_2$dhbq)(DMF)$_2$ synthesized from the reduced H$_4$Ph$_2$dhbq with Mn^{II} in layered MeOH/DMF at room temperature in air. The average particle length is 38.7 ± 18.2 μm and diameter is 4.53 ± 2.89 μm.

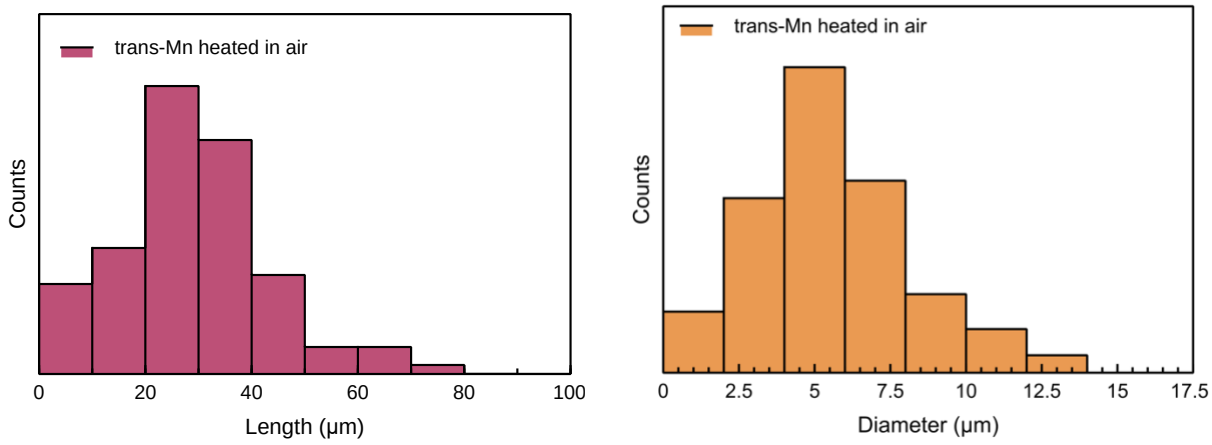

Figure S19. Particle size distributions derived from the SEM images of *trans*-Mn(Ph_2dhbq)$(DMA)_2$ synthesized from the reduced H_4Ph_2dhbq with Mn^{II} in DMA with heat in air. The average particle length is 28.8 ± 14.6 μm and diameter is 5.66 ± 2.61 μm.

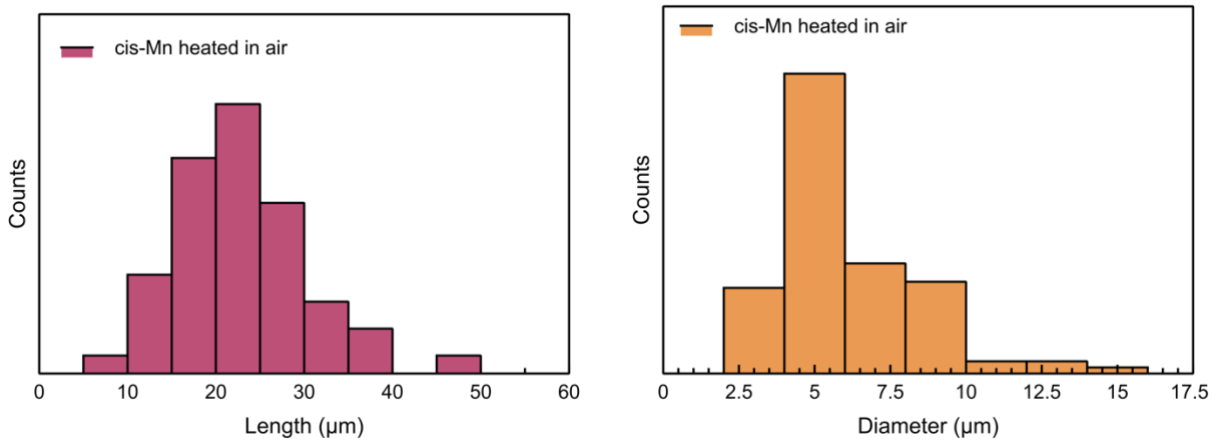

Figure S20. Particle size distributions derived from the SEM images of *cis*-Mn(Ph_2dhbq)$(DMF)_2$ synthesized from the reduced H_4Ph_2dhbq with Mn^{II} in DMF with heat in air. The average particle length is 22.9 ± 7.6 μm and diameter is 6.10 ± 2.30 μm.

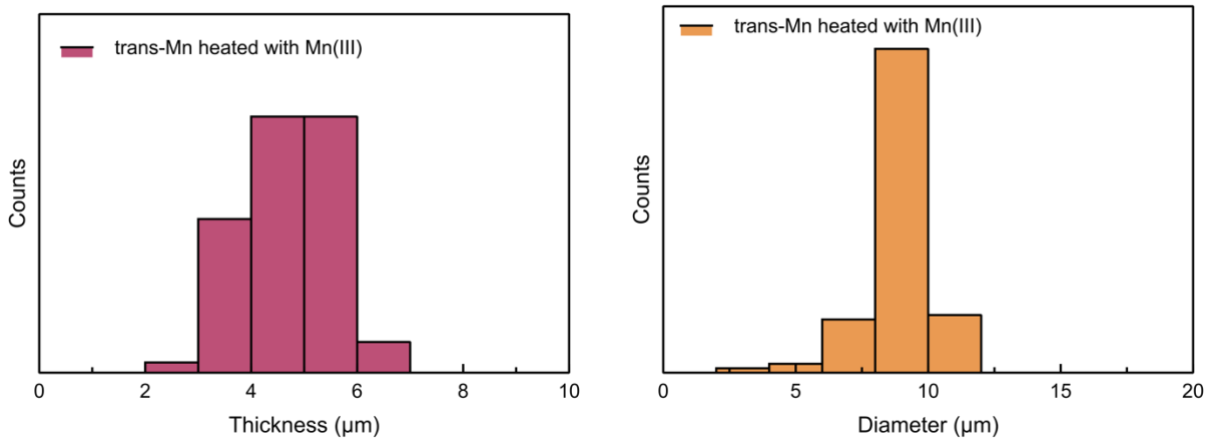

Figure S21. Particle size distributions derived from the SEM images of *trans*-Mn(Ph$_2$dhbq)(DMA)$_2$ synthesized from the reduced H$_4$Ph$_2$dhbq with Mn^{III} in DMA with heat under an inert atmosphere. The average particle thickness is 4.66 ± 0.87 μm and diameter is 8.97 ± 1.32 μm.

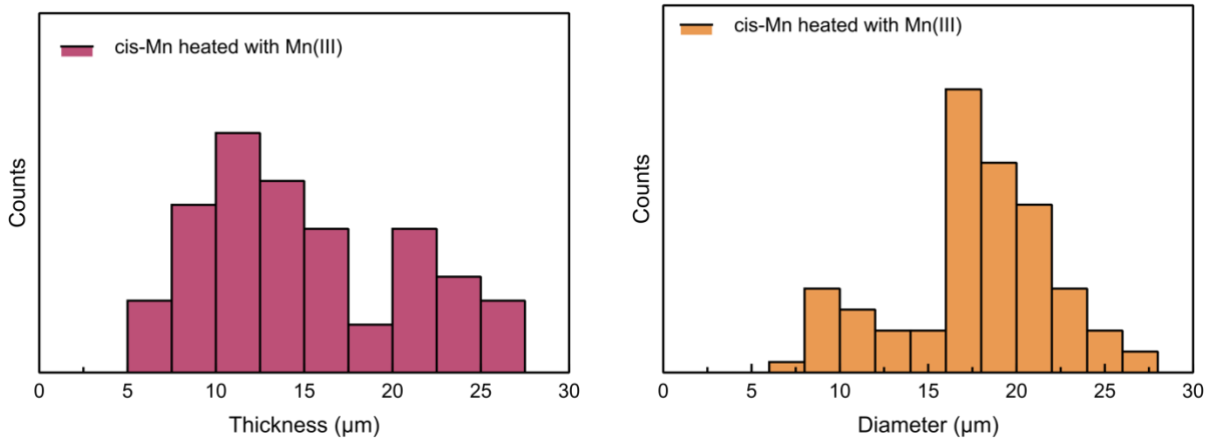

Figure S22. Particle size distributions derived from the SEM images of *cis*-Mn(Ph$_2$dhbq)(DMF)$_2$ synthesized from the reduced H$_4$Ph$_2$dhbq with Mn^{III} in DMF with heat under an inert atmosphere. The average particle thickness is 15.2 ± 5.9 μm and diameter is 17.6 ± 4.4 μm.

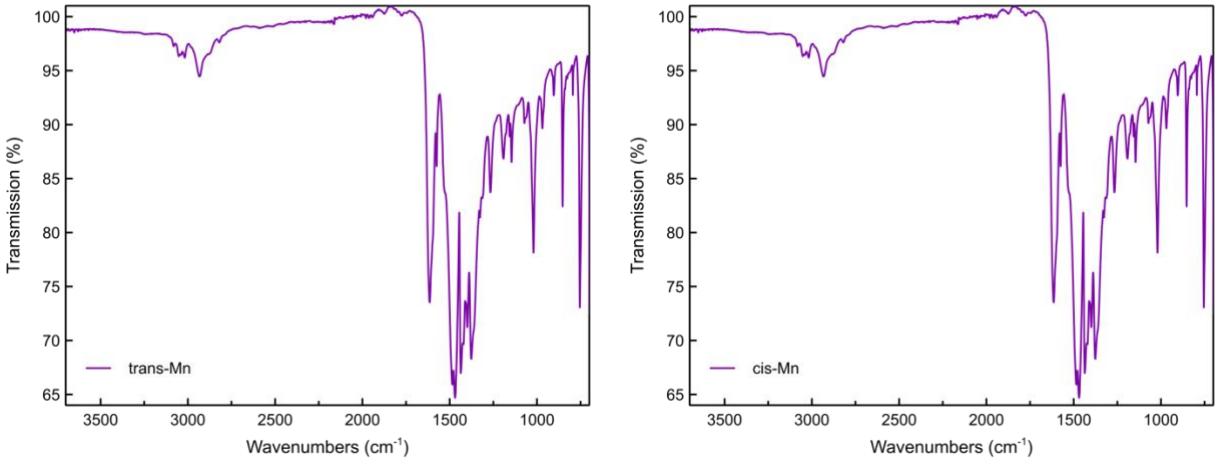

Figure S23. IR spectrum of (left) *trans*-Mn(Ph$_2$dhbq)(DMA)$_2$ and (right) *cis*-Mn(Ph$_2$dhbq)(DMF)$_2$.

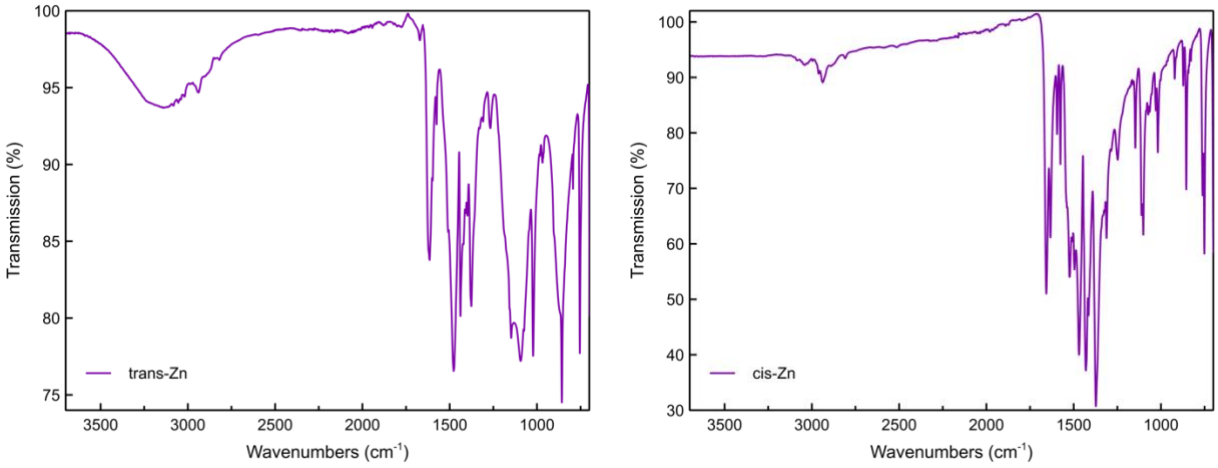

Figure S24. IR spectrum of (left) *trans*-Zn(Ph$_2$dhbq)(DMA)$_2$ and (right) *cis*-Zn(Ph$_2$dhbq)(DMF)$_2$.

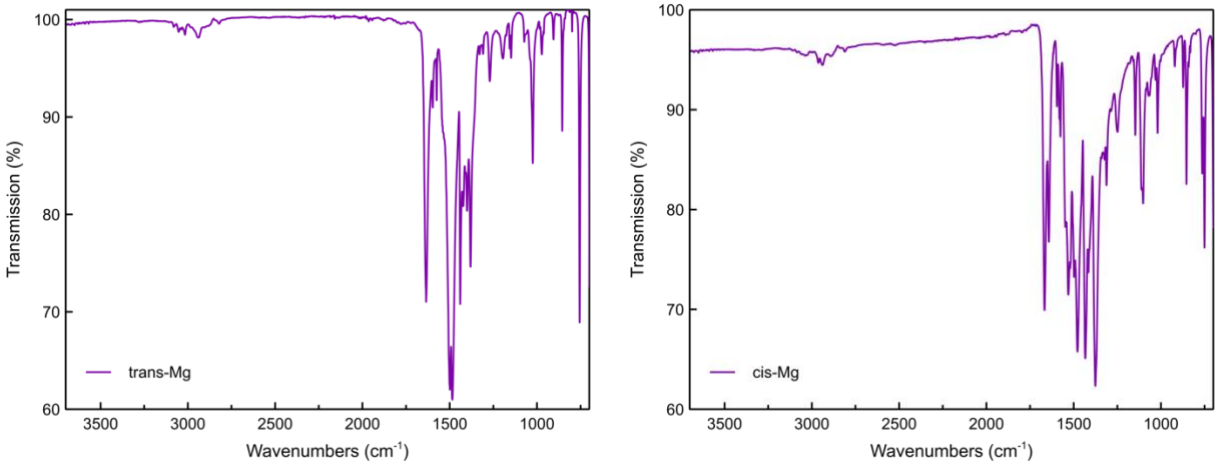

Figure S25. IR spectrum of (left) *trans*-Mg(Ph$_2$dhbq)(DMA)$_2$ and (right) *cis*-Mg(Ph$_2$dhbq)(DMF)$_2$.

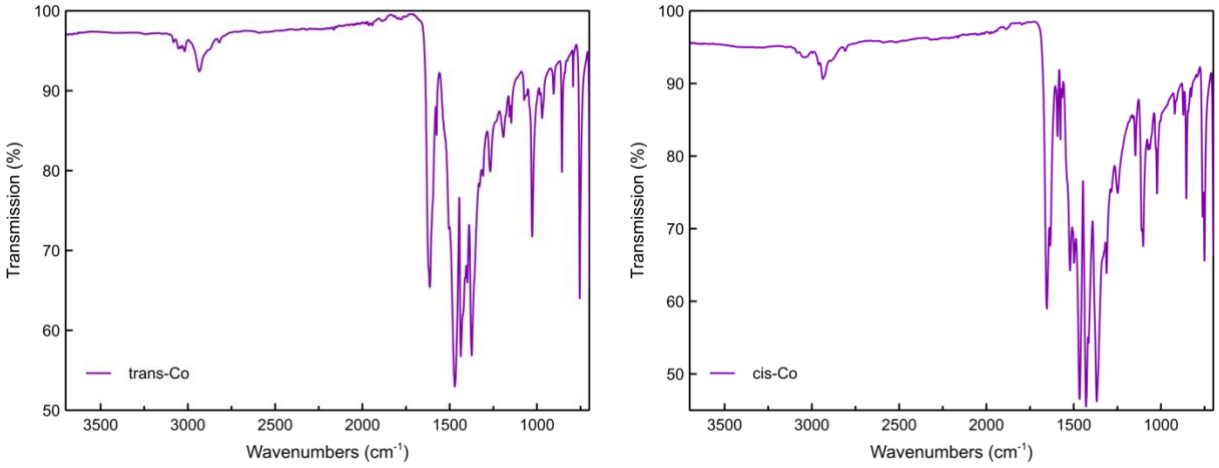

Figure S26. IR spectrum of (left) *trans*-Co(Ph$_2$dhbq)(DMA)$_2$ and (right) *cis*-Co(Ph$_2$dhbq)(DMF)$_2$.

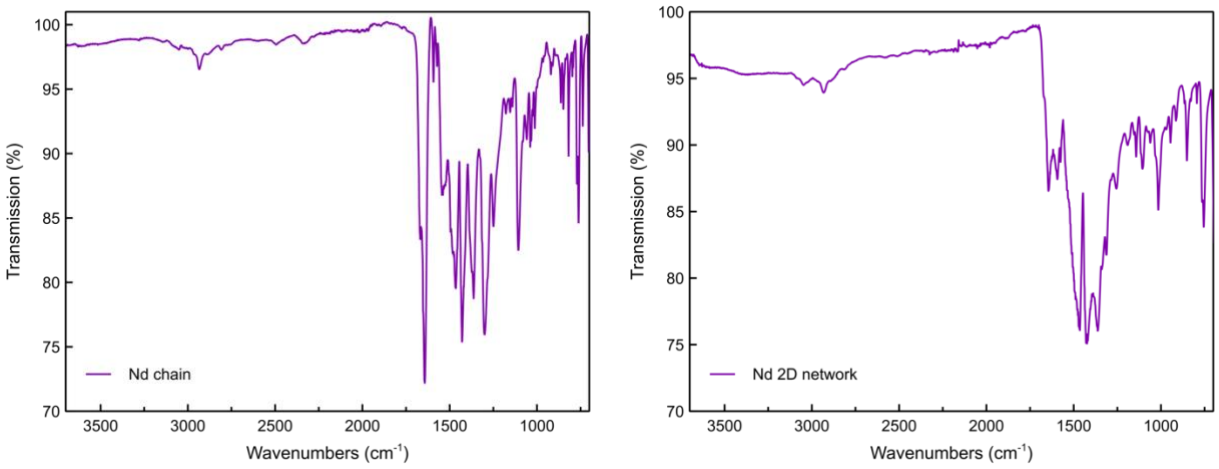

Figure S27. IR spectrum of (left) $Nd(Ph_2dhbq)(DMF)_3(NO_3)$ and (right) $Nd_2(Ph_2dhbq)_3(DMF)_6$.

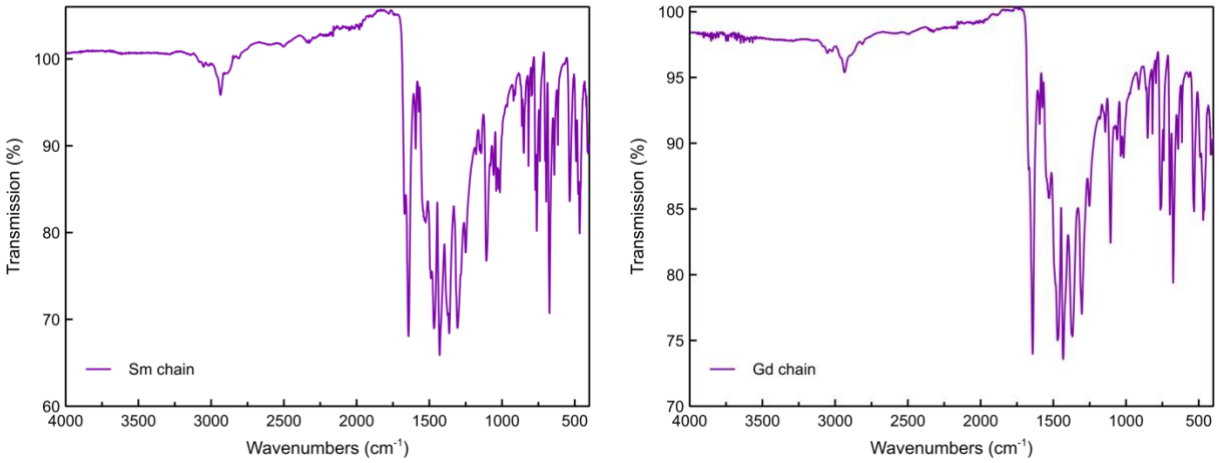

Figure S28. IR spectrum of (left) $Sm(Ph_2dhbq)(DMF)_3(NO_3)$ and (right) $Gd(Ph_2dhbq)(DMF)_3(NO_3)$.

6. References

(1) Kamin, A. A.; Moseley, I. P.; Oh, J.; Brannan, E. J.; Gannon, P. M.; Kaminsky, W.; Zadrozny, J. M.; Xiao, D. J. Geometry-Dependent Valence Tautomerism, Magnetism, and Electrical Conductivity in 1D Iron–Tetraoxolene Chains. *Chem. Sci.* **2023**, *14* (15), 4083–4090. https://doi.org/10.1039/D2SC06392A.

(2) Bruker (2007). APEX2 (Version 2.1-4), SAINT (Version 7.34A), SADABS (Version 2007/4). BrukerAXS Inc., Madison, Wisconsin, USA.

(3) Sheldrick, G. M. A Short History of SHELX. *Acta Cryst A* **2008**, *64* (1), 112–122. https://doi.org/10.1107/S0108767307043930.

(4) Sheldrick, G. M. SHELXT – Integrated Space-Group and Crystal-Structure Determination. *Acta Cryst A* **2015**, *71* (1), 3–8. https://doi.org/10.1107/S2053273314026370.

(5) SHELDRICK, G. M. SHELXL-97, Program for the Solution of Crystal Structures. *University of Göttingen, Germany.* **1997**.

(6) Sheldrick, G. M. Crystal Structure Refinement with SHELXL. *Acta Cryst C* **2015**, *71* (1), 3–8. https://doi.org/10.1107/S2053229614024218.

(7) Waasmaier, D.; Kirfel, A. New Analytical Scattering-Factor Functions for Free Atoms and Ions. *Acta Cryst A* **1995**, *51* (3), 416–431. https://doi.org/10.1107/S0108767394013292.